The *in planta* gene expression of *Austropuccinia psidii* in resistant and susceptible *Eucalyptus grandis*

Shae Swanepoel [1], Erik A. Visser [1], Louise S. Shuey [2], Sanushka Naidoo [1*]

[1] Department of Biochemistry, Genetics and Microbiology, Forestry and Agricultural Biotechnology Institute (FABI), University of Pretoria, South Africa

[2] Department of Agriculture and Fisheries, Queensland Government, Australia

*Corresponding author: sanushka.naidoo@fabi.up.ac.za

Keywords: oxalic acid; dual RNA-seq; phytohormones; host-pathogen interactions; *Austropuccinia psidii*, *Eucalyptus grandis*

Abstract

Austropuccinia psidii, commonly known as myrtle rust, is an obligate, biotrophic rust pathogen that causes rust disease on a broad host range of Myrtaceae species. *Eucalyptus grandis*, a widely cultivated hardwood Myrtaceae species, is susceptible to *A. psidii* infection, with this pathogen threatening both their natural range and various forest plantations across the world. This study aimed to investigate the *A. psidii* transcriptomic responses in resistant and susceptible *E. grandis* at four time points. RNA-seq reads were mapped to the *A. psidii* reference genome to quantify expressed genes at 12-hours post inoculation (hpi), 1-, 2- and 5-days post inoculation (dpi). A total of eight hundred and ninety expressed genes were found, of which forty-three were candidate effector proteins. These included a rust transferred protein (*RTP1*) gene, expressed in susceptible hosts at 5-dpi and a hydrolase protein gene expressed in both resistant and susceptible hosts over time. Functional categorisation of expressed genes revealed processes enriched in susceptible

hosts, including malate metabolic and malate dehydrogenase activity, implicating oxalic acid in disease susceptibility. These results highlight putative virulence or pathogenicity mechanisms employed by *A. psidii* to cause disease and provides the first insight into the molecular responses of *A. psidii* in *E. grandis* over time.

Introduction

Austropuccinia psidii (Winter) Beenken (Beenken, 2017) is an obligate biotrophic rust pathogen that causes myrtle rust on a broad host range within Myrtaceae, affecting approximately 480 species within 86 genera (Soewarto et al., 2019). Myrtle rust is considered a global pandemic, with incidence reports in North America, South America, Asia, Africa and various Oceania countries (Carnegie et al., 2010; Coutinho et al., 1998; du Plessis et al., 2017; du Plessis et al., 2019; Giblin, 2013; Kawanishi et al., 2009; Marlatt and Kimbrough, 1979; McTaggart et al., 2016; Rayachhertry et al., 1997; Roux et al., 2016; Uchida et al., 2006; Zhuang and Wei, 2011). Myrtle rust causes significant damage to growing plant leaves and shoots, causing shoot tip dieback, stunted growth and in cases of severe infection, seedling death (Glen et al., 2007). Symptoms are known to vary within and between species, with some species displaying complete resistance while others exhibit severe susceptibility (Minchinton et al., 2014).

Eucalyptus grandis is an important forestry species, valued for its wood quality and rapid growth properties (Grattapaglia et al., 2012). This economically and ecologically important hardwood species is vulnerable to various emerging pests and pathogens, including myrtle rust, which causes widespread losses to its natural and economical range. *E. grandis* is considered highly susceptible to myrtle rust infection, although some variation in disease severity exists between different genotypes (Junghans et al., 2003a). Constitutive expression of genes related to salicylic acid (SA)-

mediated responses, photosynthesis and a plethora of leucine-rich receptors was linked to resistance against myrtle rust in *E. grandis*, while these responses were limited or absent in susceptible samples (Santos et al., 2020). A recent study that combined proteomics and metabolomics to investigate the interactions between *A. psidii* and *E. grandis* implicated the phenylpropanoid pathway, photosynthetic pathway, and oxidative burst in the observed resistance against this pathogen (Sekiya et al., 2021). Plants susceptible to myrtle rust were found to exhibit similar responses, although earlier accumulation in resistant plants and more effective downstream control are the main factors separating the phenotypes (Sekiya et al., 2021). dos Santos et al. (2019) showed the importance of the cuticular waxes composition in the resistance against myrtle rust, with resistant plants having greater amounts of waxes than susceptible varieties. Moreover, susceptible *E. grandis* waxes contained hexadecenoic acid, and this compound was found to be favourable to *A. psidii*, impacting growth and germination.

There have been advances in our understanding of the putative mechanisms underlying host resistance against myrtle rust based on transcriptomic studies. Comparatively, few studies have investigated the mechanisms *A. psidii* employs to initiate host colonisation and disease. Quecine et al. (2016) highlighted the importance of cell wall degrading enzymes (CWDEs) in the success of *A. psidii*, with enzymes such as peptidases, proteases, and modification proteins involved in host susceptibility. These authors found that susceptible guava (*Psidium* guajava) infected with myrtle rust had greater abundance of pathogen-derived heat-shock proteins (HSPs), tubulin and actin proteins than what was found in the more resistant infected *Eucalyptus grandis*, suggesting an involvement of these chaperones in maintaining pathogen virulence.

Rust fungi are a complex group of plant pathogens that consist of approximately 8000 species (Aime et al., 2017). These diverse fungal pathogens have significantly larger genomes than any

other fungal species, with sizes ranging from 300 Mbp to 2 Gbp (Aime et al., 2017; Bakkeren and Szabo, 2020). Studies on rust pathogens have revealed candidate effector proteins, although to date, few of these have been functionally characterised (Petre et al., 2014). A rust pathogen of poplar (*Melampsora larici-populina*) secretes an effector protein (Mlp124357) that increases host susceptibility to bacterial and oomycete pathogens by localising to the tonoplast of host cells to facilitate infection (Madina et al., 2020). A rust transferred protein (RTP1) was identified from the broad bean rust pathogen, *Uromyces fabae,* (Kemen et al., 2005) and was found to form filaments inside the host plant to facilitate pathogen virulence during late-stage rust infection by protecting the haustorium from degradation (Kemen et al., 2013). Despite limited understanding of fungal effectors, and even more so of rust fungal effectors, recent advances in "omics" have facilitated studies on these complex organisms to unravel the role these proteins play during host colonisation and fungal proliferation.

There have been few studies investigating the molecular interactions of myrtle rust within its host plants, highlighting the need for resources that can advance our understanding of the mechanisms by which this pathogen causes disease. With the release of the *A. psidii* reference genome (Tobias et al., 2021; doi.org/10.1101/2022.04.22.489119), it is expected that many studies will emerge investigating this pathosystem. The identification of candidate effectors and virulence and pathogenicity genes highlights targets for future functional studies. The aim of this study was to investigate *A. psidii* responses in both resistant and susceptible *E. grandis*, to identify candidate effector proteins as well as pathways involved in the interactions. Elucidating the molecular mechanisms that govern these interactions will highlight novel pathogen targets for disease control and management. This is the first study to look at the molecular interactions of myrtle rust with *E. grandis* over a time series.

Materials and Methods

Austropuccinia psidii inoculation trial

Eucalyptus grandis seedlings were sourced from wild plants across their natural distribution in eastern Australia, ranging from Coffs Harbour in New South Wales to northern tropical regions of Queensland. Seedlings were grown from seed and germinated in glasshouse conditions, where temperatures ranged from 20-30ºC. The seedlings, all with at least four young leaves, were initially inoculated to determine the phenotypes. Inoculations were as reported in Swanepoel et al. (2021). The seedlings were screened for resistance and susceptibility on a scale of 1 to 5 two weeks post inoculation, where seedlings rated one were considered resistant (R-interaction) and seedlings rated five were considered susceptible (S-interaction), based on the system used in Junghans et al. (2003b). Seedlings rated R and S were selected and diseased tissues were removed. The seedlings were allowed to reshoot for eight weeks. Seedlings were inoculated (infected) with *A. psidii* urediniospores in 0.05% tween 20 with a concentration adjusted to 1×10^5 mL^{-1} or mock-inoculated with 0.05% tween 20 (control) (Swanepoel et al., 2021). Samples were collected from these seedlings at four time points (12-hours post inoculation (hpi), 1-, 2-, and 5-days post inoculation (dpi)), with three replicates per time point per phenotype, and 14 seedlings per replicate.

Data generation and annotation

Total RNA extraction was performed on inoculated and mock-inoculated frozen leaf samples as described by Naidoo et al. (2013) and Swanepoel et al. (2021). Purified RNA from three biological replicates were submitted to the Beijing Genomics Institute (BGI) for mRNA-sequencing using 50 bp paired-end Illumina HiSeq 2500, an insert size of 300 bp and a sequencing depth of 40 million reads per sample.

The host (Myburg et al., 2014) and pathogen (Tobias et al., 2021) reference genomes were downloaded from Phytozome v12.1.5 (Goodstein et al., 2011) and Zenodo (DOI:10.5281/zenodo.3567172), respectively. The reference genomes were combined to create a genome index to be used in the mapping analysis. Quality filter-passed reads were mapped to the index genome using Spliced Transcript Alignment to a Reference (STAR) v2.7.0, a universal RNA-seq aligner tool (Dobin et al., 2013) and read counts was determined using StringTie v1.3.4d Pertea et al., 2015). Read counts were imported into R v1.4.1106 (R Core Team, 2018) using tximport v1.180 (Sonesone et al., 2015). The Eukaryotic non-model Transcriptome Annotation Pipeline (EnTAP) v0.8.2 (Hart et al., 2019) was used to obtain functional annotations of the myrtle rust genome. Diamond v0.9.9 (Buchfink et al., 2015) was used to perform BLASTp similarity searches using the NCBI non-redundant protein database, RefSeq complete protein database and the UniProtKB/Swissprot database with a minimum-query coverage of 80%, minimum target coverage of 60% and a minimum e-value of 1e-05. To obtain functional gene descriptions and gene ontology (GO) terms for each *A. psidii* gene, EggNOG v0.99.1 (Huerta-Cepas et al., 2019) and InterProScan v5.25-64.0 (Jones et al., 2014) were used. To identify putative pathways involved in the *A. psidii* infection process, the protein sequences of the expressed *A. psidii* genes were annotated using GhostKOALA (Kanehisa et al., 2008) and analysed using the Kyoto Encyclopaedia of Genes and Genomes (KEGG) database.

Differential expression analysis

To identify confidently expressed *A. psidii* genes, transcripts with read counts lower than 20 in at least three libraries were filtered out, as they are considered lowly expressed. The filtered read counts were analysed using DESeq2 v 1.30.1 (Love et al., 2014). Pathogen genes were considered

significantly differentially expressed genes (DEGs) with a Benjamini & Hochberg false discovery rate (FDR) of $p < 0.05$ and when the absolute value of $\log_2$ fold change > 0.5. Comparisons between R- and S-interactions at each time point were made, where up-regulation refers to genes with greater expression in the S-interaction and down-regulation refers to genes with lower expression in the S-interaction.

Functional characterisation and identification of virulence and pathogenicity factors

To identify over-represented gene ontology (GO) biological process (BP), cellular component (CC) and molecular function (MF) *A. psidii* terms, DEGs separated into up- and down-regulated genes were used for GO enrichment using GOSeq v1.42.0 (Young et al., 2010) with a Benjamini & Hochberg FDR of $p < 0.1$. Similarly, total expressed *A. psidii* genes separated into R- and S-interaction specific expression across the time series were used for GO enrichment following the same method. GO enrichment was determined separately for BP, CC, MF, and Kyoto Encyclopaedia of Genes and Genomes (KEGG) terms. To identify putative virulence and pathogenicity factors, expressed myrtle rust genes in the R- and S-interaction throughout the time series were identified and aligned to the pathogen-host interaction (PHI) database v4.2 (Urban et al., 2020), with a minimum e-value of 1e-04 and a minimum identity of 60% to the query sequence. Additionally, the expressed genes were compared to the candidate effectors identified by Tobias et al. (2021) in the R- and S-interaction throughout the time series. The protein sequences of the expressed candidate effectors were aligned to the NCBI non-redundant protein database with default parameters. Informative hits with a minimum e-value of 1e-05 were selected for further analyses.

155 **Comparisons between *Austropuccinia psidii* transcriptome and proteome data**

156 In a previous study investigating the proteome of *A. psidii* in susceptible *P. guajava* and resistant
157 *E. grandis,* urediniospores were collected from infected fruit and leaves of *P. guajava* and *E.*
158 *grandis,* respectively (Quecine et al., 2016). The authors determined the protein abundance of these
159 samples and log ratios of susceptible relative to resistant abundance was made. Protein sequences
160 of the 340 total detected proteins captured within the urediniospores were retrieved from the
161 UniProtKB/Swiss (http://www.uniprot.org/ release Version 2021_04) with their accessions
162 (Quecine et al., 2016). The protein sequences were used to perform a Conditional Reciprocal Best
163 (CBR) BLAST (Aubry et al., 2014) against the predicted *A. psidii* proteome to identify hits that
164 are the most likely representatives of the previously identified proteins. These were then compared
165 to the total expressed *A. psidii* genes to determine which proteins corresponded with expressed
166 genes.

167 **Results**

168 **RNA sequencing, mapping and expressed *Austropuccinia psidii* genes**

169 RNA-sequencing libraries for both the R- and S-interactions included approximately 20 million
170 paired-end reads per sample at each time point (Supplementary Table 1). As expected, effectively
171 100% of mapped reads in the mock-inoculated control samples (con) mapped to the host reference
172 genome for both R- and S-interactions at each time point, confirming the quality of the mapping
173 analysis. Across the inoculated (inf) R- and S-interactions at each time point, 99.28%-100% of
174 mapped reads mapped to the host reference genome and 0.00%-0.72% of mapped reads mapped
175 to the pathogen reference genome. At 2- and 5-dpi in the resistant interaction, one and two
176 biological replicates respectively, as well as at 2-dpi in the susceptible interaction, less than 1000

reads mapped to the pathogen genome. The overall lowly mapped pathogen reads may affect downstream gene expression analysis, as the number of mapped reads may not accurately represent the *in planta* interaction between *E. grandis* and *A. psidii*. More reads mapped to the S-interaction at 5-dpi than the R interaction (Supplementary Table 1, Fig. 1). This is expected, as the S-interaction had significantly more disease symptoms than that of the R-interaction, and this may correlate with greater fungal biomass as the disease progresses in the S-interaction, resulting in the detection of more fungal RNA.

There were a total 890 confidently expressed *A. psidii* genes detected throughout the R- and S-interactions over the time series, with 683 having annotations (ca. 77%). Four hundred and twenty-four of the annotated genes had hits to hypothetical proteins (ca. 62%) and 26 genes had hits to uncharacterised proteins (ca. 4%). The remaining genes had informative annotations that may shed light on the interactions between myrtle rust and *E. grandis*. Fig. 1 shows the distribution of expressed genes across the time series. There were more expressed genes detected in the S-interaction at 12-hpi, with 418 compared to 380 in the R-interaction. The number of expressed *A. psidii* genes increased in the R-interaction to 709, while only 639 genes were expressed in the S-interaction. By 2-dpi, the number of genes significantly decreased in the R-interaction while remaining relatively stable in the S-interaction. During late-stage infection at 5-dpi, the number of genes in the S-interaction rose to 888, representing ca. 99% of the total expressed genes detected. Comparatively, the number of genes expressed in the R-interaction decreased dramatically to 234. The total number of expressed genes has similar distributions to the percentage of mapped reads (Fig. 1). This is likely related to the power of detection at each time point in both the resistant and susceptible hosts.

Of the top ten most highly expressed *A. psidii* genes, seven were common between the R- and S-interactions (Table 1 and Supplementary Table 2 and 3, respectively). Three of these genes are among the candidate effectors defined by Tobias et al. (2021). Moreover, five of these genes are among the list of DEGs at 5-dpi. Unfortunately, these genes had no successful annotations. It is imperative to determine the identity of these genes and the role they play during the interaction, as it may shed light on the pathogenicity and virulence of *A. psidii*. This is particularly true of the genes uniquely highly expressed in the S-interaction. Similarly, when investigating the top 100 most highly expressed genes, comparisons between the R- and S-interaction revealed 78 genes in common between interactions and 22 genes unique to either the R- or S-interaction.

When analysing the total expressed genes using KEGG, 529 genes (ca. 59%) had successful annotations. The functional categories included "genetic information processing" (ca. 47%), "carbohydrate metabolism" (ca. 8%), "cellular processes" (ca. 6%) and "energy metabolism" (ca. 5%). KEGG enrichment revealed involvement of "2-oxocarboxylic acid metabolism", "biosynthesis of amino acids" and "glyoxylate and dicarboxylate metabolism" among others (Supplementary Table 4).

Differentially expressed *Austropuccinia psidii* genes

Differential gene expression analysis was performed to determine the differences in gene expression between the R- and S-interactions. *A. psidii* DEGs were considered up-regulated when expression was greater in the S-interaction compared to the R-interaction. Since there were only 890 confidently expressed *A. psidii* genes, there were very few DEGs. No DEGs were identified at 12-hpi and 2-dpi. At 1-dpi, *APSI_H004.3230* was significantly differentially expressed (DE) between the R- and S-interactions, with expression lower in the S-interaction ($\log_2$ (fold change)

221 = -7.2). This gene did not have successful hits when functionally annotated, so putative functions
222 are unknown. At 5-dpi, 11 genes were up-regulated with expression greater in the S-interaction
223 and 15 genes were down-regulated with expression lower in the S-interaction. Supplementary
224 Table 5 shows the annotations of the 26 DEGs at 5-dpi.

225 **Gene ontology enrichment analysis**

226 GO enrichment analyses were performed to identify putative pathways involved in the interactions
227 between *E. grandis* and *A. psidii*. There were no significantly over-represented terms upon GO
228 enrichment when analysing the DE dataset. This is expected due to the small number of DEGs.
229 When analysing the total expressed gene space, 188 over-represented GO BP terms were identified
230 across the R- and S-interaction over the time series (Fig. 2, Supplementary Table 6). These terms
231 were predominantly associated with cellular processes, including terms such as translation, cellular
232 protein metabolic process, and cellular biosynthetic process. These processes were shared among
233 both the R- and S-interaction over time. Terms that were unique to the S-interaction included
234 energy processes such as ATP synthesis, energy coupled proton transport and mitochondrial ATP
235 synthesis. Additionally, oxoacid metabolic processes and organic acid metabolic processes were
236 also unique to the S-interaction. Terms unique to the R-interaction included glyoxylate cycle and
237 metabolic process, dicarboxylic acid biosynthesis and cellular aldehyde metabolic process.

238 Twenty-three over-represented MF terms were identified across the R- and S-interactions. Terms
239 unique to the S-interaction included malate dehydrogenase activity and saccharopine
240 dehydrogenase activity and terms involved in transcription were unique to the R-interaction
241 (Supplementary Fig. 1). When investigating the CC category, 77 over-represented terms were

identified. Terms involving cellular processes were over-represented, including transcription and translation (Supplementary Fig. 2).

Austropuccinia psidii **pathogenicity and virulence factors**

The 890 confidently expressed myrtle rust genes aligned using the PHI database v4.2 (Urban et al., 2020). Genes with hits greater than 60% identity to the subject query and those implicated in virulence and pathogenicity were retained for further analysis. The R-interaction had 24 genes with successful hits (Table 2, Supplementary Table 7) while the S-interaction had 32 genes with successful hits to the subject query (Table 2). Hits unique to the S-interaction included a gene involved in cAMP signalling (*Gib2*, *APSI_P008.17130, APSI_H002.12341*) and a gene encoding a putative pyridoxal 5'-phosphate synthase subunit (*PdxS*, *APSI_P009.17505*). Additionally, while the R- and S-interaction shared common hits, the S-interaction had expression of more orthologs of certain genes. These included expression of an additional *cyclophilin* (*CPA1*, *APSI_P005.10514*), *tubulin alpha-1 chain* (*TUB1*, *APSI_H010.14180*), *conserved actin protein* (*ActA*, *APSI_H003.4114*), *hypothetical protein* (*MGG_00383, APSI_H021.3806*), and a *beta2-tubulin* housekeeping gene (*APSI_H018.10108*). Hits shared between resistant and susceptible interactions included *heat shock proteins* (*HSPs*), a transcription factor gene identified in *Magnaporthe oryzae* and a gene encoding *3-isopropylmalate dehydratase* (Table 2).

Analysis of the candidate effector proteins identified by Tobias et al. (2021) revealed a total of 43 expressed genes in the present study (Fig. 3A, Supplementary Table 8). The S-interaction had seven uniquely expressed candidate effectors over the course of infection, two at 2-dpi and five at 5-dpi (Supplementary Table 8). The expression of these genes was not observed in the R-interaction. To investigate putative virulence and pathogenicity of these candidates, the protein

sequences were subjected to a BLASTp on the NCBI non-redundant database. Seventeen of the 43 expressed genes had successful hits to proteins from other organisms, predominantly rust fungi. Many of these hits corresponded with hypothetical or uncharacterised proteins (Supplementary Table 9). Interestingly, five hits corresponded with informative hits (Table 3). A *small subunit ribosomal protein S10e* (*APSI_H017.8250*), a *rust transferred protein 1* (*RTP1*, *APSI_P008.18155*) and a *non-catalytic module family protein* (*APSI_H007.8820*) were uniquely expressed in the S-interaction. A *small subunit ribosomal protein S10e* (*APSI_P005.11212*) and a *hydrolase 76 protein* (*APSI_P004.3557*) were expressed in both interactions. The expression of these genes in the R- and S-interaction across the time series is represented by Fig. 3B.

Comparisons of *Austropuccinia psidii* transcriptome and proteome

To gain a deeper understanding of the key mechanisms governing the interaction between *A. psidii* and its hosts, the proteome results obtained by Quecine et al. (2016) was compared to the RNA-seq results obtained in the present study. There were 200 active and 140 obsolete entries (ca. 59%) for the proteins identified by Quecine et al. (2016) when retrieving protein sequences from UniProtKB/Swiss. This may be due to improvements in the genomes of the organisms, making some entries obsolete or redundant. CRB BLAST results revealed 387 predicted *A. psidii* hits that are most putative representatives of the proteins identified in the proteome study (Supplementary Table 10). From this, 82 genes were expressed in our transcriptome study (Table 4, Supplementary Table 11). These included *HSPs* that were either uniquely expressed in susceptible *P. guajava* or in greater abundance in *P. guajava* relative to resistant *E. grandis* (Quecine et al., 2016). There was greater expression of these *HSPs* in the R-interaction at 1-dpi, with expression in the S-interaction greater at 5-dpi. Other genes identified included those encoding for calnexin, enolase,

pyruvate kinase, spermidine synthase and tubulin beta chain proteins. Many *hypothetical proteins* genes were identified within our dataset, with these uniquely abundant in *P. guajava* or *E. grandis* (Table 4).

Discussion

Due to the obligate biotrophic nature of rust fungi, there have been limited studies on molecular genetics underlying the pathogen molecular dialogue with the host plant. With improving next generation sequencing, omics studies have facilitated the study of these complex organisms, highlighting candidate pathogenicity genes that can be studied using heterologous systems (Bakkeren and Szabo, 2020). This has broadened our understanding of rust disease and aided in development of efficient control strategies.

The present study investigated the molecular responses of the pandemic biotype of *A. psidii* in resistant and susceptible *E. grandis*. This was achieved by pooling 14 highly heterozygous seedlings in three replicates per phenotype per time point. Despite the high heterozygosity of host material within and between samples, host responses were previously observed to be consistent between biological replicates (Swanepoel et al., 2021) and similarly, pathogen expression showed consistency between hosts over time. However, key differences between hosts were observed, including unique expression of candidate effectors in susceptible hosts as well as pathogenicity and virulence factors and pathways potentially contributing to disease. The results of this study are similar to that of Quecine et al. (2016), revealing that *A. psidii* might employ similar mechanisms to elicit host disease in different plant species.

Over the course of infection, the number of reads mapping to the pathogen genome decreased in the resistant (R) interaction. This suggests that over the course of infection, the R-interaction

308 successfully suppresses the growth and development of the pathogen, thereby reducing the number
309 of pathogen transcripts observed in the analysis. The number of reads mapping to the reference
310 genome in the susceptible (S) interaction significantly increases over the course of infection,
311 suggesting that the S-interaction does not mount an effective defence response to prevent the
312 proliferation of the pathogen. This is observed in the interaction between *A. psidii* and *M.*
313 *quinquenervia*, where the number of reads mapping to the resistant hosts was 0% compared to 2%
314 in the susceptible hosts, suggesting only susceptible hosts facilitate the growth of the pathogen at
315 5-dpi (Hsieh et al., 2018). This is observed in the present study, where the greatest number of
316 expressed genes in the analysis were identified in the S-interaction at 5-dpi (n = 888). These results
317 are further supported by Tobias et al. (2018) in which resistant hosts actively respond to *A. psidii*
318 infection, while susceptible hosts lack a sufficient, coordinated response, potentially contributing
319 to the number of transcripts observed. This corroborates the results obtained in our previous studies
320 on *E. grandis* responses to *A. psidii* (Swanepoel et al., 2021), where the infection on susceptible
321 leaves presented as severe pustules of urediniodspores progressing over the course of infection

322 **Shared virulence and pathogenicity factors**

323 In the present study, analysis of expressed candidate effectors revealed a *family 76 hydrolase*
324 *protein* gene expressed in both the R- and S-interaction across the time series. Furthermore, a
325 putative *family 61 glycoside hydrolase protein* was DE at 5-dpi, with expression significantly
326 greater in the R- compared to the S-interaction. These are classes of cell wall degrading enzymes
327 (CWDE) that are employed by pathogens to degrade preformed barriers. Hydrolase proteins are
328 known to contribute to degradation of plant cell walls in other rust fungi (Cooper et al., 2016; Wu
329 et al., 2019). Greater expression of these genes in the R-interaction is unexpected. It is possible

330 that the pathogen is over-expressing these CWDE in resistant hosts to compensate for the effective
331 preformed barriers that are preventing pathogen entry into the host plant (dos Santos et al., 2019).
332 In the interaction with *A. psidii* and *E. grandis,* it was found that callose deposition was enriched
333 across the time series in resistant *E. grandis,* while this was poorly coordinated in the susceptible
334 hosts, only enriched at 5-dpi (Swanepoel et al., 2021). Thus, entry into the plant cells could occur
335 with relative ease and more rapidly in susceptible hosts, as preformed barriers may not be adequate
336 to prevent pathogen entry. Tobias et al. (2018) supports this, where infected resistant *S. luehmannii*
337 was found to have greater expression of a secondary cell wall synthesis gene that encodes beta-
338 1,4-xylosyltransferase compared to susceptible hosts. This suggests that preformed barriers are
339 more prominent in resistant hosts. These results highlight a prominent area for future work.

340 Among the genes found in the interaction were numerous *HSPs*. HSPs are known to be involved
341 in chaperoning the folding of proteins, but they also function to protect the cell from stress,
342 including heat stress, fluctuations in pH and oxidative stress (Pandey et al., 2018; Tiwari et al.,
343 2015). Two *HSPs 90* (*APSI_P013.4275, APSI_H009.11612*) were identified as potential virulence
344 factors in both the R- and S-interaction when compared to PHI-base. HSP90 is involved in complex
345 protein folding processes and is vital to the functioning of the organism (Nathan et al., 1997).
346 Previous studies on rust fungi virulence and pathogenicity factors have identified a plethora of
347 HSPs enriched in susceptible hosts, suggesting that these proteins play crucial roles in facilitating
348 plant disease (Cooper et al., 2016; Quecine et al., 2016). Quecine et al. (2016) identified various
349 pathogen-derived HSPs during the interactions with *A. psidii,* with more HSPs identified in
350 susceptible *P. guajava* than in resistant *E. grandis*. This is further supported by Song et al. (2011),
351 where numerous HSPs were isolated from the haustoria of *Puccinia triticina,* a wheat leaf rust

352 fungus. The expression of *HSPs* in this study suggests a significant role of these proteins in the
353 interaction between *A. psidii* and *E. grandis*.

354 Amino acid biosynthesis and metabolism pathways were significantly enriched in both the R- and
355 S-interactions. The gene encoding the enzyme 3-isopropylmalate dehydratase, involved in the
356 biosynthesis of leucine, was identified as a putative pathogenicity factor when compared to the
357 PHI-base in both interactions (Table 2). Moreover, one of these proteins was identified in the
358 urediniospores of *P. guajava* and *E. grandis,* where abundance was greater in susceptible *P.*
359 *guajava* than in resistant *E. grandis* (log ratio = 0.81, Table 4, Supplementary Table 11, Quecine
360 et al., 2016). This implicates this enzyme in the disease process of *A. psidii* and tags it as an
361 important pathway for disease control strategies.

362 **Virulence and pathogenicity factors uniquely expressed in susceptible hosts**

363 *PdxS* was found to contribute to viability, stress tolerance and virulence of the gram-negative
364 bacterial pathogen, *Actinobacillus pleuopneumoniae,* which causes pleuropneumonia respiratory
365 disease (Xie et al., 2017). *PdxS* catalyses the production of pyridoxal 5'-phosphate (PLP), a
366 biochemically active form of vitamin B6 (Eliot and Kirsch, 2004). *PdxS* mutants exhibited
367 abnormal morphology, with craters on their surfaces, suggesting that adequate production of PLP
368 by *PdxS* is required for normal cell morphology (Xie et al., 2017). PLP is a cofactor for
369 phosphorylation, playing a key role in many physiological processes, including amino acid
370 biosynthesis and metabolism. In a study conducted by Song et al. (2011) on *P. triticina,* a Pdx1
371 protein was isolated from the haustoria during interactions with wheat. Moreover, a pyridoxine
372 biosynthesis protein was more abundant in susceptible *P. guajava* than resistant *Eucalyptus* when
373 investigating the proteome of *A. psidii* infected hosts (Quecine et al., 2016)

Rust transferred protein 1 may manipulate the reactive oxygen species production

Five expressed *A. psidii* candidate effector genes had successful annotations when subjected to BLAST analysis (Table 3). A *rust transferred protein* (*RTP1*) was identified in the S-interaction at 5-dpi, with expression of this gene not detected in the R-interaction. This protein, initially identified in *Uromyces fabae,* was found to localise in the extra-haustoria matrix during early stages of infection as well as inside the host cell cytoplasm as disease progresses and the haustoria matures. This suggests RTP1 plays a crucial role in maintaining the biotrophic lifestyle with host plants (Kemen et al., 2005; Kemen et al., 2013). It was found that as the haustoria matures over the course of infection, high concentrations of RTP1p can be found within the host cytoplasm (Kemen et al., 2013). As a result, cyclosis of host nucleus and chloroplasts is inhibited, with the authors suggesting this cessation is the result of accumulation of RTP1p (Kemen et al., 2013).

Oxalic acid may manipulate host oxidative and phytohormone pathways

In the present study, genes involved in malate dehydrogenase, oxoacid metabolism and malate metabolism were identified (Supplementary Fig. 1 and Fig. 2). Malate dehydrogenase is an enzyme that catalyses the reaction of malate to oxaloacetate, a precursor molecule for oxalic acid production. The accumulation of oxalic acid produces an acidic environment within the host plant to facilitate crucial fungal mechanisms of infection, which includes the secretion of virulence factors (Lovat et al., 2019). Oxalic acid is known to reduce plant oxidative burst responses and produce an acidic environment in the host cells to facilitate disease in host plants (Cessna et al., 2000, Laurent et al., 1993). In the interaction between *Castanea* spp. and the chestnut blight pathogen *Cryphonectria parasitica,* oxalate (oxalic acid) is produced by the pathogen, reducing the host cellular pH to promote the functioning of crucial fungal enzymes that manipulate oxidative

burst (Lovat et al., 2019). A previous study investigating *E. grandis* responses to *A. psidii* found significant involvement of the oxidative burst response in defence response (Swanepoel et al., 2021). The plant-type HR was prominent in resistant hosts at 2- and 5-dpi while susceptible hosts only responded with HR at 5-dpi. This suggests that despite both hosts regulating and mounting respiratory burst responses, the susceptible hosts lacked the ability to convert these into HR. This may be due to the involvement of pathogen secreted virulence factor such as malate dehydrogenase and oxalic acid.

In the same study, the authors found the putative involvement of phytohormones in the host responses to *A. psidii* (Swanepoel et al., 2021). This included salicylic acid (SA), jasmonic acid (JA), ethylene (ET) and abscisic acid (ABA) enriched in both the R- and S-interactions, as well as brassinosteroids (BR) enriched only in the R-interaction. Applications of oxalic acid to *Brassica napus* L. has been shown to affect phytohormone signalling within the plant (Liang et al., 2009). Proteins associated with phytohormone pathways including JA and ET were increased following applications of oxalic acid. Despite the evidence suggesting that SA is not directly affected in the presence of oxalic acid, it was found that pathways mediated by the phytohormone were decreased (Liang et al., 2009). Therefore, we hypothesise that *A. psidii* may produce oxalic acid to manipulate the phytohormone crosstalk within susceptible *E. grandis*.

While comparisons between the proteome (Quecine et al., 2016) and the transcriptome of *A. psidii* provides valuable insights into the molecular mechanisms governing the interactions of *A. psidii* with its hosts, it is important to remember that timing of collection of materials for analysis plays a role in the outcome of the results obtained. Furthermore, the study conducted on the proteome isolated urediniospores of *P. guajava* and *E. grandis*, while the present study isolated fungal RNA from whole leaf samples. Different infection structures and stages can affect the results obtained.

Additionally, Quecine et al. (2016) considered the differences that exist between different species, while the present study aimed to determine the differences that exist within *E. grandis* provenances. Therefore, the results obtained in the comparisons need to be further validated to confirm how the proteins and genes found contribute to disease susceptibility.

Conclusions

The interaction between resistant and susceptible *E. grandis* and *A. psidii* share similarities, with the timing of infection crucial to the disease progression, highlighted by unique pathogen genes expressed solely in the S-interaction at 5-dpi. Several pathways were shown in this study, putatively contributing to the molecular dialogue with *E. grandis*. This is the first study to investigate the expression of *A. psidii* genes *in planta* over a time series. Through this, several candidate *A. psidii* genes and pathways have been identified for future functional studies that investigate their roles in the interaction with *E. grandi*s. This includes the uniquely expressed *RTP1* gene, various *HSP* genes, *CWDE* genes as well as the putative involvement of oxalic acid in pathogenicity. In conclusion, this reveals genes and pathways that may be manipulated to control the devastating effects this pathogen has on native and introduced Myrtaceae species.

Data availability statement

The data have been uploaded to the NCBI under bioproject PRJNA763498.

Author contributions

SS performed data analysis, interpretation of results and drafted the manuscript. EAV assisted with data analysis, interpretation and drafting of the manuscript. LSS conceived the study, performed experiments to obtain the data and evaluated the manuscript. SN conceived of and obtained

funding for the study, assisted in interpreting the biological responses, and drafting of the manuscript. All authors approve the submitted version.

Funding

This work was supported by the South African National Research Foundation (NRF) Y-rated Grant to SN (UID105767) and post-doctoral support to LSS. The authors acknowledge the funding from the Technology Innovation Agency (TIA) of South Africa through the Forest Molecular Genetics Cluster Program to SN, SS and EAV. Opinions and conclusions arrived of the authors do not reflect those of the NRF and other funding agencies.

Literature Cited

Aime, M. C., McTaggart, A. R., Mondo, S. J., and Duplessis, S. 2017. Phylogenetics and phylogenomics of rust fungi. Adv. Genet. 100:267-307.

Aubry, S., Kelly, S., Kümpers, B. M. C., Smith-Unna, R. D., and Hibberd, J. M. 2014. Deep evolutionary comparison of gene expression identifies parallel recruitment of trans-factors in two independent origins of C4 photosynthesis. PLoS Genet. 10:e1004365.

Bakkeren, G., and Szabo, L. J. 2020. Progress on molecular genetics and manipulation of rust fungi. Phytopathol. 110:532-543.

Beenken, L. 2017. *Austropuccinia*: A new genus name for the myrtle rust *Puccinia psidii* placed within the redefined family Sphaerophragmiaceae (Pucciniales). Phytotaxa 297:53-61.

Buchfink, B., Xie, C., and Huson, D. H. 2015. Fast and sensitive protein alignment using DIAMOND. Nat. Methods 12:59-60.

Carnegie, A. J., Lidbetter, J. R., Walker, J., Horwood, M. A., Tesoriero, L., Glen, M., and Priest, M. J. 2010. *Uredo rangelii*, a taxon in the guava rust complex, newly recorded on Myrtaceae in Australia. Australas. Plant. Pathol. 39:463-466.

Cessna, S. G., Sear, V. E., Dickman, M. B., and Low, P. S. 2000. Oxalic acid, a pathogenicity factor for *Sclerotinia sclerotiorum*, suppresses the oxidative burst of the host plant. The Plant Cell 12:2191-2199.

Cooper, B., Campbell, K. B., Beard, H. S., Garret, W. M., and Islam, N. 2016. Putative rust fungal effector proteins in infected bean and soybean leaves. Phytopathol. 106:491-499.

Coutinho, T. A., Wingfield, M. J., Alfenas, A. C., and Crous, P. W. 1998. *Eucalyptus* rust: A disease with the potential for serious international implications. Plant Dis. 82:819-825.

Dobin, A., Davis, C. A., Schlesinger, F., Drenkow, J., Zaleski, C., Jha, S., Batut, P. B., Chaisson, M., and Gingeras, T. R. 2013. STAR: Ultrafast universal RNA-seq aligner. Bioinformatics 29:15-21.

dos Santos, I. B., Lopes, M. d. S, Bini, A. P., Tschoeke, B. A. P., Verssani, B. A. W., Figueredo, E. F., Cataldi, T. R., Marques, J. P. R., Silva, L. D., Labate, C. A. and Quecine, M. C. 2019. The *Eucalyptus* cuticular waxes contribute in preformed defense against *Austropuccinia psidii*. Front. Plant Sci. 9:1978.

du Plessis, E., McTaggart, A. R., Granados, M. J., Wingfield, M. J., Roux, J., Ali, M. I. M., Pegg, G. S., Makinson, J., and Purcell, M. 2017. First report of myrtle rust caused by *Austropuccinia psidii* on *Rhodomyrtus tomentosa* (Myrtaceae) from Singapore. Plant Dis. 101:1676

du Plessis, E., Granados, G. M., Barnes, I., Ho, W. H., Alexander, B. J. R., Roux, J., and McTaggart, A. R. 2019. The pandemic strain of *Austropuccinia psidii* causes myrtle rust in New Zealand and Singapore. Australas. Plant. Pathol. 48:253-256.

Eliot, A. C., and Kirsch, J. F. 2004. Pyridoxal phosphate enzymes: Mechanistic, structural, and evolutionary considerations. Annu. Rev. Biochem. 73:383-415.

Fernandez, D., Tisserant, E., Talhinhas, P., Azinheria, H., Vieira, A., Petitot, A. S., Loureiro, A., Poulain, J., Da Silva, C., Silva, M. D. C., and Duplessis, S. 2012. 454-pyrosequencing of *Coffea arabica* leaves infected by the rust fungus *Hemileia vastatrix* reveals in planta-expressed pathogen-secreted proteins and plant functions in a late compatible plant-rust interaction. Mol. Plant. Pathol. 13:17-37.

Giblin, F. 2013. Myrtle rust report: New Caledonia. Assessment of myrtle rust situation in New Caledonia. University of the Sunshine Coast Maroochydore, Queensland, Australia.

Glen, M., Alfenas, A. C., Zauza, E. A. V., Wingfield, M. J., and Mohammed, C. 2007. *Puccinia psidii*: A threat to the Australian environment and economy – A review. Australas. Plant. Pathol. 36:1-16.

Goodstein, D. M., Shu, S., Howson, R., Neupane, R., Hayes, R. D., Fazo, J., Mitros, T., Dirks, Q., Hellsten, U., Putnam, N., and Rokhsar, D. S. 2011. Phytozome: A comparative platform for green plant genomics. Nucleic Acids Res. 40:D1178-1186.

Grattapaglia, D., Vaillancourt, R. E., Shepard, M., Thumma, B. R., William, F., Külheim, C., Potts, B. M., and Myburg, A. A. 2012. Progress in Myrtaceae genetics and genomics: *Eucalyptus* as the pivotal genus. Tree Genet. Genomes. 8:463-508.

Handschumacher, R. E., Harding, M. W., Rice, J., Drugge, R. J., and Speicher, D. W. 1984. Cyclophilin: A specific cytosolic binding protein for cyclosporin A. Sci. 226:544-547.

Hart, A. J., Ginzburg, S., Xu, M., Fisher, C. R., Rahmatpur, N., Mitton, J. B., Paul, R., and Wegrzyn, J. L. 2019. EnTAP: Bringingfaster and smarter functional annotation to non-model eukaryotic transcriptomes. Mol. Ecol. Resour. 20:591-604.

Hsieh, J-F., Chuah, A., Patel, H. R., Sandu, K. S., Foley, W. J., and Külheim, C. 2018. Transcriptome profiling of *Melaleuca quinquenervia* challenged by myrtle rust reveals differences in defense responses among resistant individuals. Phytopathol. 108:495-509.

Huerta-Cepas, J., Szklarczyk, D., Heller, D., Hernández-Plaza, A., Forslund, S. K., Cook, H., Mende, D. R., Letunic, I, Rattei, T., Jensen, L. J., von Mering, C., and Bork P. 2019. eggnog 5.0: A hierarchical, functionally and phylogenetically annotated orthology resource based on 5090 organisms and 2502 viruses. Nucleic Acids Res. 47:D309-D314.

Jones, P., Binns, D., Chang, H-F., Fraser, M., Li, W., McAnulla, C., McWilliam, H., Maslen, J., Mitchell, A., Nuka, G., Pesseat, S., Quinn, A. F., Sangrador-Vegas, A., Scheremetjew, M., Yong, S-Y., Lopez, R., and Hunter, S. 2014. InterProScan 5: Genome-scale protein function classification. Bioinformatics. 30:1236-1240.

Junghans D. T., Alfenas, A. C., Brommonschenkel, S. H., Oda, S., Mello, E. J., and Grattapaglia, D. 2003a. Resistance to rust (*Puccinia psidii* Winter) in *Eucalyptus*: Mode of inheritance and mapping of a major gene with RAPD markers. Theor. Appl. Genet. 108:175-180.

Junghans, D. T., Alfenas, A. C., and Maffia, L. A. 2003b. Escala de notas para quantificação da ferrugem em *Eucalyptus*. Fitopatol. Bras. 28:184-188.

Kanehisa, M., Araki, M., Goto, S., Hattori, M., Hirakawa, M., Itoh, M., Katayama, T., Kawashima, S., Okuda, S., Tokimatsu, T., and Yamanishi, Y. 2008. KEGG for linking genomes to life and the environment. Nucleic Acid Res. 36:480-484.

526 Kawanishi, T., Uematsu, S., Kakishima, M., Kagiwada, S., Hamamoto, H., Horie, H., and
527 Namba, S. 2009. First report of rust disease on ohia and the causal fungus, *Puccinia*
528 *psidii,* in Japan. J. Gen. Plant. Pathol. 75:428-431.
529 Kemen, E., Kemen, A. C., Rafiqi, M., Hempel, U., Mendgen, K., Hahn, M., and Voegele, R. T.
530 2005. Identification of a protein from rust fungi transferred from haustoria into infected
531 plant cells. Mol. Plant. Microbe. Interact. 18:1130-1139.
532 Kemen, E., Kemen, A. C., Ehlers, A., Voegele, R. T., and Mendgen, K. 2013. A novel structural
533 effector from rust fungi is capable of fibril formation. Plant J. 75:767-780.
534 Kingsbury, J. M., Yang, Z., Ganous, T. M., Cox, G. M., and McCusker, J. H. 2004. Novel
535 chimeric spermidine synthase-saccharopine dehydrogenase gene (*SPE3-LYS9*) in the
536 human pathogen *Cryptococcus neoformans*. Eukaryot. Cell 752:763.
537 Kretschmer, M., Damoo, D., Djamei, A., and Kronstad, J. 2020. Chloroplasts and plant
538 immunity: Where are the fungal effectors? Pathogens 9:19.
539 Laurent, L., Susan, R., Heinstein, P. F., and Low, P. S. 1993. Characterization of the
540 oligogalacturonide-induced oxidative burst in cultured soybean (*Glycine max*) cells. Plant
541 Physiol. 102:233-240.
542 Liang, Y., Strelkov, S. E., and Kav, N. N. V. 2009. Oxalic acid-mediated stress responses in
543 *Brassica napus* L. Proteomics 9:3156-3173.
544 Lovat, C-A., Donnelly, D. J., and Doğmuş-Lehtijärvi, H. T. 2019. Mechanisms and
545 metabolomics of the host-pathogen interactions between Chestnut (*Castanea species*) and
546 Chestnut blight (*Cryphonectria parasitica*). For. Pathol. 49:e12562.
547 Love, M. I., Huber, W., and Anders, S. 2014. Moderated estimation of fold change and
548 dispersion for RNA-seq data with DESeq2. Genom. Biol. 15:550.

549 Madina, M. H., Rahman, M. S., Huang, X., Zhang, Y., Zheng, H., and Germain, H. 2020. A
550 poplar rust effector protein associates with protein disulfide isomerase and enhances plant
551 susceptibility. Biology. 9:294.
552 Marlatt, R. B., and Kimbrough, J. W. 1979. *Puccinia psidii* on *Pimenta dioica* in south Florida.
553 Plant Dis. Rep. 63:510-512.
554 McTaggart, A. R., Roux, J., Granados, G. M., Gafur, A., Tarrigan, M., Santhakumar, P., and
555 Wingfield, M. J. 2016. Rust (*Puccinia psidii*) recorded in Indonesia poses a threat to
556 forests and forestry in South-East Asia. Australas. Plant. Pathol. 45:83-89.
557 Minchinton, E. J., Smith, D., Hamley, K., and Donald, C. 2014. Myrtle rust in Australia. Acta.
558 Hortic. 89-90.
559 Naidoo, R., Ferreira, L., Berger, D. K., Myburg, A. A., and Naidoo, S. 2013. The identification
560 and differential expression of *Eucalyptus grandis* pathogenesis-related genes in response
561 to salicylic acid and methyl jasmonate. Front. Plant. Sci. 4:43.
562 Nathan, D. F., Vos, M. H., and Lindquist, S. 1997. *In vivo* functions of the *Saccharomyces*
563 *cerevisiae* Hsp90 chaperone. PNAS 94:12949-12956.
564 Pandey, V., Singh, M., Pandey, D., and Kumar, S. 2018. Integrated proteomics, genomics,
565 metabolomics approaches reveal oxalic acid as pathogenicity factor in *Tilletia indica*
566 inciting Karnal bunt disease of wheat. Sci. Rep. 8:7826.
567 Pertea, M., Pertea, G. M., Antonescu, C. M., Chang, T-C., Mendall, J. T., and Salzberg, S. L.
568 2015. StringTie enables improved reconstruction of a transcriptome from RNA-seq reads.
569 Nat. Biotechnol. 33:290-295.
570 Petre, B., Joly, D. L., and Duplessis, S. 2014. Effector proteins of rust fungi. Front. Plant. Sci.
571 5:416.

572 Puthoff, D. P., Neelam, A., Enrenfriend, M. L., Scheffler, B. E., Ballard, L., Song, Q., Campbell,
573 K. B., Cooper, B., and Tucker, M. L. 2008. Analysis of expressed sequence tags from
574 *Uromyces appendiculatus* hyphae and haustoria and their comparison to sequences from
575 other rust fungi. Phytopathol. 98:1126-1135.
576 Quecine, M. C., Leite, T. F., Bini, A. P., Regiani, T., Franceschini, L. M., Budzinski, I. G. F.,
577 Marques, F. G., Labate, M. T. V., Guidetti-Gonzalez, S., Moon, D. H., and Labate, C. A.
578 2016. Label-free quantitative proteomic analysis of *Puccinia psidii* uredospores reveals
579 differences of fungal populations infecting *Eucalyptus* and guava. PLoS One
580 11:e0145343.
581 R Development Core Team. 2018. R: A language and environment for statistical computing.
582 RDC Team, ed. R Foundation for Statistical Computing, Vienna, Austria 1:409.
583 Rayachhetry, M. B., Elliot, M. L., and Van, T. K. 1997. Natural epiphytotic of the rust *Puccinia*
584 *psidii* on *Melaleuca quinquenervia* in Florida. Plant Dis. 81:831.
585 Roux, J., Granados, G. M., Shuey, L., Barnes, I., Wingfield, M. J., and McTaggart, A. R. 2016.
586 A unique genotype of the rust pathogen, *Puccinia psidii*, on Myrtaceae in South Africa.
587 Australas. Plant. Pathol. 45:645-652.
588 Santos, S. A., Vidigal, P. M. P., Guimarães, L. M. S., Mafia, R. G., Templeton, M. D., and
589 Alfenas, A. C. 2020. Transcriptome analysis of *Eucalyptus grandis* genotypes reveals
590 constitutive overexpression of genes related to rust (*Austropuccinia psidii*) resistance.
591 Plant Mol. Biol. 104:339-357.
592 Sekiya, A., Marques, F. G., Leite, T. F., Cataldi, T. R., de Moraes, F. E., Pinheiro, A. L. M.,
593 Labate, M. T. V., and Labate, C. A. 2021. Network analysis combining proteomics and

metabolomics reveals new insights into early responses of *Eucalyptus grandis* during rust infection. Front. Plant. Sci. 11:604849.

Singh, K., Winter, M., Zouhar, M., and Ryšánek, P. 2018. Cyclophilins: Less studied proteins with critical roles in pathogenesis. Phytopathol. 108:6-14.

Soewarto, J., Giblin, F., and Carnegie, A. J. 2019. *Austropuccinia psidii* (myrtle rust) global host list. Version 4. Australian network for plant conservation, Canberra, ACT. http://www.anpc.asn.au/myrtle-rust . Accessed 20 November 2020.

Sonesone, C., Love, M. I., and Robinson, M. D. 2015. Different analyses or RNA-seq: Transcript-level estimates improve gene-level inferences. F1000Research 4:1521.

Song, X., Rampitsch, C., Soltani, B., Mauthe, W., Linning, R., Banks, T., McCallum, B., and Bakkeren G. 2011. Proteome analysis of wheat leaf rust fungus, *Puccinia triticina,* infection structures enriched for haustoria. Proteomics 11:944-963.

Swanepoel, S., Oates, C. N., Shuey, L. S., Pegg, G. S., and Naidoo, S. (2021). Transcriptome analysis of *Eucalyptus grandis* implicates brassinosteroid signaling in defense against myrtle rust (*Austropuccinia psidii*). Front. For. Glob. Change 4:778611.

Tiwari, S., Thankur, R., and Shankar, J. 2015. Role of heat-shock proteins in the cellular function and in the biology of fungi. Biotechno. Res. Int. 2015:132635-132635.

Tobias, P. A., Guest, D. I., Külheim, C., and Park, R. F. 2018. De novo transcriptome study identifies candidate genes involved in resistance against *Austropuccinia psidii* (myrtle rust) in *Syzygium luehmannii* (riberry). Phytopathol. 108:627-640.

Tobias, P. A., Schwessinger, B., Deng, C. H., Wu, C., Dong, C., Sperschneider, J., Jones, A., Lou, Z., Zhang, P., and Sandhu, K. S. 2021. *Austropuccinia psidii,* causing myrtle rust,

has a gigabase-sized genome shaped by transposable elements. G3-Genes. Genom. Genet. 11:jkaa015.

Uchida, J., Zhong, S., and Killgore, E. 2006. First report of a rust disease on Ohia caused by *Puccinia psidii* in Hawaii. Plant Dis. 90:524.

Urban, M., Cuzick, A., Seager, J., Wood, V., Rutherford, K., Venkatech, S. Y., De Silva, N., Martinez, M. C., Pedro, H., Yates, A. D., Hassani-Pak, K., and Hammond-Kosack, K. E. 2020. PHI-base: The pathogen-host interactions database. Nucleic Acids Res. 48:D613-D620.

Viaud, M., Brunet-Simon, A., Brygoo, Y., Pradier, J. M., and Levis, C. 2003. Cyclophilin A and calcineurin functions investigated by gene inactivation, cyclosporin A and cDNA arrays approaches in the phytopathogenic fungus *Botrytis cinerea.* Mol. Microbiol. 50:1451-1465.

Wang, Y., Shen, G., Gong, J., Shen, D., Whittington, A., Qing, J., Treloar, J., Boisvrt, S., Zhang, Z., Yang, C., and Wang, P. 2014. Noncanonical Gβ Gib2 is a scaffolding protein promoting cAMP signaling through functions of Ras1 and Cac1 proteins in *Cryptococcus neoformans*. J. Biol. Chem. 289:12202-12216.

Wu, W., Nemri, A., Blackman, L. M., Catanzariti, A-M., Sperschneider, J., Lawrence, G. J., Dodds, P. N., Jones, D. A., and Hardham, A. R. 2019. Flax rust infection transcriptomics reveals a transcriptional profile that may be indicative for rust *Avr* genes. PLoS One 14e0226106.

Xie, F., Li, G., Wang, Y., Zhang, Y., Zhou, L., Wang, C., Liu, S., Liu, S., and Wang, C. 2017. Pyridoxal phosphate synthases PdxS/PdxT are required for *Actinobacillus pleuropneumoniae* viability, stress tolerance and virulence. PLoS One 12:e0176374.

639 Young, M. D., Wakefield, M. J., Smyth, G. K., and Oshlack, A. 2010. Gene ontology analysis
640 for RNA-seq: Accounting for selection bias. Genom. Biol. 11:R14.
641 Zhang, H., Liu, K., Zhang, X., Tang, W., Wang, J., Guo, M., Zhao, Q., Zheng, X., Wang, P., and
642 Zhang, Z. 2011. Two phosphodiester genes, *PDEL* and *PDEH,* regulate development and
643 pathogenicity by modulating intracellular cyclic AMP levels in *Magnaporthe oryzae.*
644 PLoS One 6:e17241.
645 Zhang, H., Ma, H., Xie, X., Ji, J., Dong, Y., Du, Y., Tang, W., Zheng, X., Wang, P., and Zhang,
646 Z. 2014.Comparative proteomic analyses reveal that the regulators of G-protein signaling
647 proteins regulate amino acid metabolism of the rice blast fungus *Magnaporthe oryzae*.
648 Proteomics 14:21-22.
649 Zhuang, J. Y., and Wei, S. X. 2011. Additional materials for the rust flora of Hainan Province,
650 China. Mycosystema 30:853-860.
651
652
653
654
655
656
657

Tables

Table 1. Expressed *Austropuccinia psidii* PHI-annotated genes in the R-interaction with percentage identity greater than 60% and implications in pathogenicity and virulence.

Gene	FPKM[a]		Description	Differential expression[b]	Candidate effector[c]
	Resistant	Susceptible			
APSI_H016.15346	114834.2	63263.2	-	Down	Yes
APSI_P008.17159	42222.1	42296.8	-	-	No
APSI_P015.13113	35201.5	38433.9	-	-	Yes
APSI_P016.16372	42274.5	68001.6	-	Up	Yes
APSI_P016.16375	40218.8	57525.0	-	Up	No
APSI_P017.12412	43208.9	35281.8	-	Down	No
APSI_P017.12428	29575.3	25499.5	-	Down	No

[a] Average FPKM across the time series

[b] Significant differential expression at 5-dpi during colonisation of susceptible relative to resistant hosts

[c] Candidate effectors based on the parameters defined by Tobias et al. (2021)

FPKM = fragment per kilobase million

668 **Table 2**. Expressed *Austropuccinia psidii* pathogen-host interactions database (PHI)-annotated genes in the
669 R- and S-interaction with percentage identity greater than 60% and implications in pathogenicity and
670 virulence

Query identity	Interaction	PHI base gene description	Identity (%)	Mutant phenotype
APSI_H008.9528	R+S	Cyclophillin	68	0
APSI_H009.11612	R+S	Ubiquitous chaperone, heat shock protein 90	64	0
APSI_H010.13601	R+S	regulators of G-protein (GTP-binding protein) signalling (RGS) proteins/homocitrate synthase	64	0
APSI_H010.13652	R+S	Tubulin alpha-1 chain	78	1; 2
APSI_H010.13828	R+S	Glycogen synthase kinase, central signal regulator involved in the stress-responsive mechanism	69	1
APSI_H012.10735	R+S	Serine/threonine kinase	80	1
APSI_P001.5636	R+S	Heat shock protein	68	1
APSI_P001.5642	R+S	Heat shock protein	68	1
APSI_P001.5837	R+S	Uncharacterised protein	70	0
APSI_P001.6093	R+S	Calcium permease	61	0
APSI_P001.6880	R+S	Hypothetical protein	74	0

APSI_P002.14583	R+S	regulators of G-protein (GTP-binding protein) signalling (RGS) proteins/homocitrate synthase	68	0
APSI_P002.15004	R+S	glycogen synthase kinase	70	0; 1
APSI_P002.15358	R+S	Tubulin alpha-1 chain	74	1; 2
APSI_P003.1647	R+S	Cytochrome C peroxidase precursor	63	0
APSI_P003.2172	R+S	3-Isopropylmalate dehydratase	62	1
APSI_P011.231	R+S	Acetolactate synthase	65	1
APSI_P013.4275	R+S	Ubiquitous chaperone, heat shock protein 90	70	0
APSI_P014.1429	R+S	transcription factor	62	1
APSI_P015.13025	R+S	Mitochondrial elongation factor Tu	63	0
APSI_P015.13172	R+S	Pyruvate kinase	61	0; 1
APSI_P017.12437	R+S	Conserved actin protein	90	0
APSI_P018.7518	R+S	Beta2-tubulin housekeeping gene	85	0
APSI_P020.4950	R+S	Bifunctional enzyme adenylosuccinate (ADS) lyase	77	0
APSI_H003.4114	S	Conserved actin protein	81	0

APSI_H018.10108	S	Beta2-tubulin housekeeping gene	85	0
APSI_P005.10514	S	Cyclophillin	68	0
APSI_P008.17130	S	Scaffolding Protein Promoting cAMP Signalling	80	0
APSI_H002.12341	S	Scaffolding Protein Promoting cAMP Signalling	80	0
APSI_H021.3806	S	Hypothetical protein	70	0
APSI_P009.17505	S	pyridoxal 5'-phosphate synthase subunit PdxS	67	0
APSI_H010.14180	S	Tubulin alpha-1 chain	76	1; 2

671 0 = reduced virulence; 1 = loss of pathogenicity; 2 = lethal

672 R = genes unique to resistant interaction; S = genes unique to susceptible interaction; R+S = genes expressed in both resistant and
673 susceptible interactions

674

675

676

677

678

679

680

681

682 **Table 3.** Informative protein BLAST results for the expressed candidate *Austropuccinia psidii* effectors in
683 R- and S-interaction identified on the non-redundant NCBI database.

Candidate effector	Interaction	Accession	Identity (%)	Description	E-value[a]
APSI_P005.11212	R+S	KNZ48236.1	81.5	Small subunit ribosomal protein S10e	3.55E-82
APSI_P004.3557	R+S	KAA1090934.1	75.9	Hydrolase 76 protein	7.44E-136
APSI_H017.8250	R+S	KNZ48236.1	82.2	Small subunit ribosomal protein S10e	5.49E-83
APSI_P009.18155	S	AFI13823.1	43.8	Rust transferred protein 1	2.13E-50
APSI_H007.8820	S	XP_007403659.1	38.7	Non-catalytic module family EXPN	1.23E-38

684 R = genes unique to resistant interaction; S = genes unique to susceptible interaction; R+S = genes expressed in both resistant and
685 susceptible interactions

686

687

688

689

690 **Table 4.** Expressed *Austropuccinia psidii* genes from comparisons to proteomic data obtained by Quecine

691 et al. (2016).

Gene ID	Description	Log ratio (ApG/ApE)[a]	Log fold change (SI/RI)[b]			
			12-hpi	1-dpi	2-dpi	5-dpi
APSI_H002.12538	-	-0.84	0.00	0.24	0.61	0.87
APSI_P002.14830	-	0.22	0.00	0.00	0.00	1.65
APSI_P015.13025	-	ApGuava	0.00	-3.09	0.19	0.70
APSI_P004.3474	3-isopropylmalate dehydrogenase	0.81	0.49	-0.71	-1.59	1.54
APSI_H009.11558	ATP synthase subunit alpha, mitochondrial	0.24	0.00	1.17	3.57	2.39
APSI_H005.1677	2-isopropylmalate synthase	0.21	-3.42	-0.60	0.00	0.70
APSI_P002.15726	2-methylcitrate dehydratase	0.3	2.80	-0.76	-0.41	0.85
APSI_P007.14326	3-isopropylmalate dehydrogenase	0.81	-3.33	0.19	0.32	-0.72
APSI_H004.3682	40S ribosomal protein S7	-0.38	0.00	0.00	3.11	2.80
APSI_H001.6084	Acetyl-CoA carboxylase	ApEucalyptus	1.56	1.18	-0.32	-0.75
APSI_H003.4114	Actin	0.09	1.73	0.00	0.00	1.15
APSI_P017.12437	Actin	0.09	0.00	-2.32	1.43	2.06
APSI_H007.8988	Adenosylhomocysteinase	-0.01	-2.84	0.00	-0.32	0.98
APSI_H014.2045	Arabinitol dehydrogenase 1	0.18	0.00	0.00	0.20	1.22
APSI_H015.423	Arginyl-tRNA synthetase	0.11	0.00	0.59	0.00	0.44
APSI_H004.3499	Aspartate aminotransferase, mitochondrial	0.31	0.00	2.45	2.38	1.00
APSI_P004.2874	Aspartate aminotransferase, mitochondrial	0.31	-4.63	-4.06	0.09	2.46
APSI_P011.364	ATP synthase subunit beta, mitochondrial	0.14	0.94	-1.98	0.08	2.33

APSI_H014.2180	Calnexin	-0.4	0.37	-2.34	0.00	0.86
APSI_P005.10461	Calnexin	-0.4	-0.76	-1.37	-0.49	2.34
APSI_P005.10288	Chlorophyll synthesis pathway protein	0.18	0.37	-1.44	0.00	0.74
APSI_P016.16045	Elongation factor 2	0	-1.55	-1.17	3.01	2.74
APSI_P016.16081	Elongation factor 2	0	0.00	-1.71	1.45	2.69
APSI_H008.9525	Enolase	0.21	0.00	2.44	0.00	0.72
APSI_P005.10519	Enolase	0.21	0.00	-2.32	1.20	1.47
APSI_P010.11580	Eukaryotic translation initiation factor 3 subunit F	0.13	-1.64	0.41	0.06	-0.35
APSI_H014.2368	Fatty acid synthase subunit beta	ApEucalyptus	0.00	0.00	0.00	0.00
APSI_P005.10846	Fatty acid synthase subunit beta	ApEucalyptus	-0.59	-1.69	-0.82	0.36
APSI_H003.4176	Glucose-regulated protein	0.08	0.00	1.86	0.00	0.42
APSI_P017.12534	Glucose-regulated protein	0.08	0.00	0.18	1.44	0.57
APSI_P008.16892	Glutamate dehydrogenase	0.14	0.00	-1.46	3.52	0.59
APSI_P010.11420	Heat shock 70kda protein 4	0.49	0.00	-3.15	2.06	2.69
APSI_P010.11427	Heat shock 70kda protein 4	0.49	0.56	-2.92	1.67	3.11
APSI_P013.4275	Heat shock protein 83	0.1	-1.53	-1.10	1.40	1.15
APSI_H022.14	Heat shock protein HSS1	0.08	-4.43	-0.32	4.02	2.33
APSI_P009.17506	Heat shock protein HSS1	0.08	-0.15	-0.54	1.38	2.63
APSI_P001.5636	Heat shock protein SSB	0.17	-3.65	0.01	1.50	3.38
APSI_P001.5642	Heat shock protein SSB	0.17	-1.73	-0.02	1.18	3.37
APSI_H009.11612	Heat-shock protein 90	0.1	-1.37	0.23	2.27	1.73
APSI_H001.6204	Hsp70-like protein	0.3	0.00	3.92	1.51	2.42
APSI_P002.14610	Hsp70-like protein	0.3	0.00	0.34	2.32	-0.08
APSI_P008.17020	Hypothetical protein	ApEucalyptus	1.16	-2.20	-0.03	0.54
APSI_H016.15678	Hypothetical protein	ApGuava	0.00	0.00	1.54	0.66

APSI_H001.6960	Hypothetical protein	0.43	0.00	1.86	2.17	0.10
APSI_P014.1140	Hypothetical protein	0.35	1.87	2.30	1.69	1.76
APSI_H003.4994	Hypothetical protein	-0.09	0.00	0.00	1.43	1.98
APSI_P014.1093	Hypothetical protein	-0.09	0.00	1.24	0.97	2.08
APSI_P001.5930	Hypothetical protein	ApEucalyptus	2.73	3.47	1.44	0.18
APSI_H018.10185	Hypothetical protein	ApGuava	1.96	0.00	-1.14	0.01
APSI_H016.15562	Hypothetical protein	0.36	0.00	-0.24	0.00	2.01
APSI_P010.11387	Hypothetical protein	-0.17	-0.38	0.88	-1.28	-0.94
APSI_H006.15165	Hypothetical protein	-0.05	-3.58	1.01	2.07	0.83
APSI_P009.17824	Hypothetical protein	ApGuava	0.00	-1.98	2.17	1.28
APSI_P006.9484	Hypothetical protein	ApGuava	0.00	0.00	0.92	1.06
APSI_P003.1597	Hypothetical protein	ApGuava	0.00	0.04	-1.04	0.56
APSI_P011.239	Hypothetical protein	-0.21	2.28	-1.36	-4.68	-0.79
APSI_P011.268	Hypothetical protein	0.53	3.14	-3.06	1.95	0.62
APSI_P019.8310	Hypothetical protein	0.43	0.00	0.00	1.54	0.10
APSI_P011.233	Hypothetical protein	ApGuava	0.00	0.05	2.88	1.73
APSI_P016.16382	Hypothetical protein	0.16	-0.51	-0.92	0.52	2.77
APSI_H017.8116	Hypothetical protein	0.03	0.00	-0.60	0.00	0.50
APSI_H017.8250	Hypothetical protein	ApGuava	0.00	0.00	0.00	1.22
APSI_P012.9011	Kinesin family member C1	0.06	1.45	1.05	1.40	2.81
APSI_H001.6292	Malate dehydrogenase, NAD-dependent	0.56	0.00	-1.26	2.08	1.75
APSI_P003.1614	Malate dehydrogenase, NAD-dependent	0.56	0.00	1.40	-0.49	1.72
APSI_H013.5798	Minichromosome maintenance protein 4	ApGuava	1.17	-1.35	1.58	-0.08

APSI_P010.11499	Minichromosome maintenance protein 6	0	-2.30	2.95	1.20	-0.37
APSI_P001.6720	Polyubiquitin-A	ApEucalyptus	-0.31	-0.22	-0.64	0.37
APSI_P017.12651	Polyubiquitin-A	ApEucalyptus	0.00	-1.44	0.00	1.41
APSI_H009.11705	Protein transporter SEC23	0.06	0.00	1.24	1.44	0.30
APSI_P013.4176	Protein transporter SEC23	0.06	0.00	2.49	0.91	0.40
APSI_H016.15523	Putative histone H9	ApEucalyptus	0.00	-3.77	1.43	0.39
APSI_P015.13172	Pyruvate kinase	ApGuava	-0.59	0.00	0.00	-0.29
APSI_P005.10979	RuvB-like helicase 1	ApGuava	0.37	-3.25	1.45	1.05
APSI_P016.16384	Secretory pathway GDP dissociation inhibitor 1	0.68	0.00	0.29	0.00	0.39
APSI_P018.7791	Spermidine synthase	ApGuava	0.00	1.07	0.31	0.29
APSI_P007.14016	T-complex protein 1 subunit alpha	-0.12	0.00	-1.62	0.00	-0.04
APSI_H006.15105	Translation initiation factor eIF-3	-0.11	0.00	0.00	0.00	0.28
APSI_H018.10108	Tubulin beta chain	0.34	0.00	0.00	0.00	0.72
APSI_P018.7518	Tubulin beta chain	0.34	0.00	-1.09	0.00	0.38
APSI_P002.15126	Uncharacterized protein	ApGuava	0.00	1.21	2.57	0.65
APSI_P007.13634	Vacuolar protein 8	ApGuava	-1.52	-0.54	-0.72	2.30

692 [a] Log ratio of ApGuava relative to ApEucalyptus (Quecine et al., 2016); [b] Log fold change of susceptible relative to

693 resistant *E. grandis*

694 ApG = *Austropuccinia psidii* guava; ApE = *Austropuccinia psidii E. grandis;* SI = S-interaction; RI = R-interaction.

695

696

697

698

699

Fig. 1. The mapping statistics and the number of total expressed *Austropuccinia psidii* genes over the time series. Lines represent the percentage of mapped reads (primary y-axis) in the resistant (blue) and the susceptible (pink) interactions, error bars represent the standard error of the mean. The bars represent the total number of expressed genes (secondary y-axis) in the resistant (blue) and susceptible (pink) interactions. A total of 890 expressed genes were identified through RNA-seq analysis. The x-axis represents the time in days post inoculation.

Fig. 2. Over-represented gene ontologies (GO) in the biological processes (BP) category of total expressed *Austropuccinia psidii* genes in both the R- and S-interaction over the time series, where the colour scale represents the false discovery rate (FDR) adjusted p-value and grey represents absence of the term. GO analysis identified 188 over-represented BP terms, the heatmap represents the top 70 terms in relation to the lowest FDR value. R = resistant interaction; S = susceptible interaction; hpi = hours post inoculation; dpi = days post inoculation.

Fig. 3. The expression of *Austropuccinia psidii* effector genes. (A) The number of expressed *Austropuccinia psidii* candidate effectors. Blue represents the genes expressed in the R-interaction, green represents expressed genes between the R- and S-interaction, and pink represents effector genes expressed in the S-interaction. (B) The expression of patterns of *Austropuccinia psidii* effectors genes in both the resistant and susceptible *Eucalyptus grandis* interactions over the time series. Genes with known annotations are labelled. The colour gradient represents the expression values of a measure of FPKM ranging from the minimum to maximum expression values, where white represents genes that are not expressed. FPKM = fragments per transcript million; hpi = hours post inoculation; dpi = days post inoculation; R = resistant interaction; S = susceptible interaction.

Supplementary material

Fig. S1. Over-represented gene ontologies (GO) in the molecular function (MF) category. The heatmap shows enriched terms of the total expressed *Austropuccinia psidii* genes in both the R- and S-interaction over the time series, where the colour scale represents the false discovery rate (FDR) adjusted p-value and grey represents the absence of the term. GO analysis identified 23 over-represented MF terms. R = resistant interaction; S = susceptible interaction; hpi = hours post inoculation; dpi = days post inoculation.

Fig. S2. Over-represented gene ontologies (GO) in the cellular component (CC) category. The heatmap shows enriched terms of the total expressed *Austropuccinia psidii* genes in both the R- and S-interaction over the time series, where the colour scale represents the false discovery rate (FDR) adjusted p-value and grey represents the absence of the term. GO analysis identified 77 over-represented CC terms. R = resistant interaction; S = susceptible interaction; hpi = hours post inoculation; dpi = days post inoculation.

Supplementary Table 1: The mapping statistics of the dual RNA-seq of *Eucalyptus grandis* and *Austropuccinia psidii.*

Supplementary Table 2: The top 100 most highly expressed *Austropuccinia psidii* genes in the resistant interaction, as a measure of FPKM values.

Supplementary Table 3: The top 100 most highly expressed *Austropuccinia psidii* genes in the susceptible interaction, as a measure of FPKM values.

Supplementary Table 4: Over-represented KEGG terms of total expressed *Austropuccinia psidii* genes representing FDR values.

743 **Supplementary Table 5:** Differentially expressed gene list at 5-dpi.

744 **Supplementary Table 6:** Over-represented gene ontologies (GO) in the biological processes (BP)
745 category of total expressed *Austropuccinia psidii* genes representing FDR values.

746 **Supplementary Table 7:** Table S7: Expressed *Austropuccinia psidii* pathogen-host interaction
747 database (PHI)-annotated genes in the R- and S-interaction with percentage identity greater than
748 60% and implications in pathogenicity and virulence

749 **Supplementary Table 8:** The expressed candidate *Austropuccinia psidii* effectors representing
750 FPKM values.

751 **Supplementary Table 9:** The top ten BLAST results for expressed candidate effectors.

752 **Supplementary Table 10:** The CRB BLAST results with target proteins identified in a previous
753 proteome study.

754 **Supplementary Table 11:** The expressed genes from the CRB BLAST results.

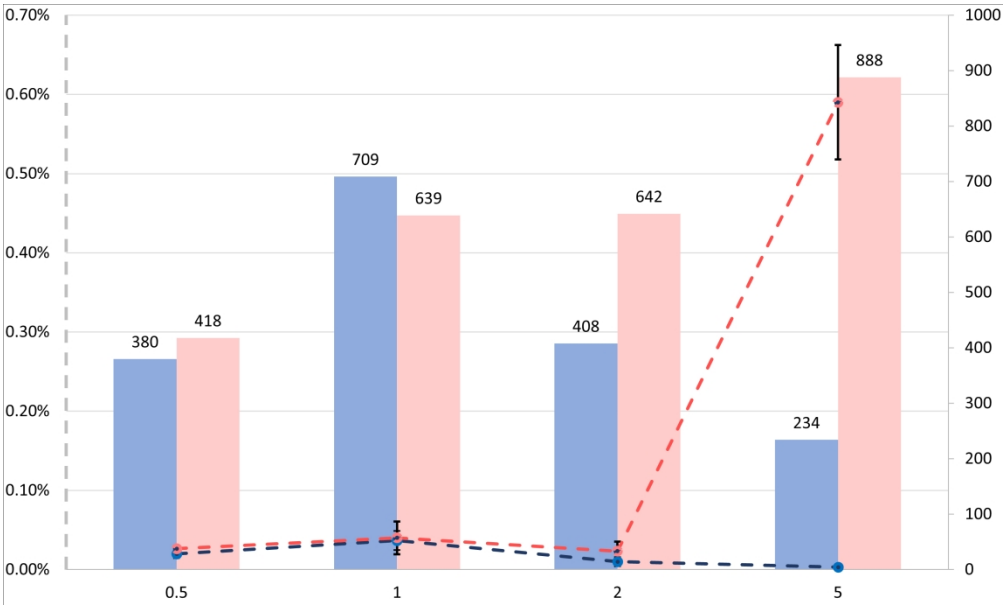

Fig. 1. The mapping statistics and the number of total expressed Austropuccinia psidii genes over the time series. Lines represent the percentage of mapped reads (primary y-axis) in the resistant (blue) and the susceptible (pink) interactions, error bars represent the standard error of the mean. The bars represent the total number of expressed genes (secondary y-axis) in the resistant (blue) and susceptible (pink) interactions. A total of 890 expressed genes were identified through RNA-seq analysis. The x-axis represents the time in days post inoculation.

237x142mm (330 x 330 DPI)

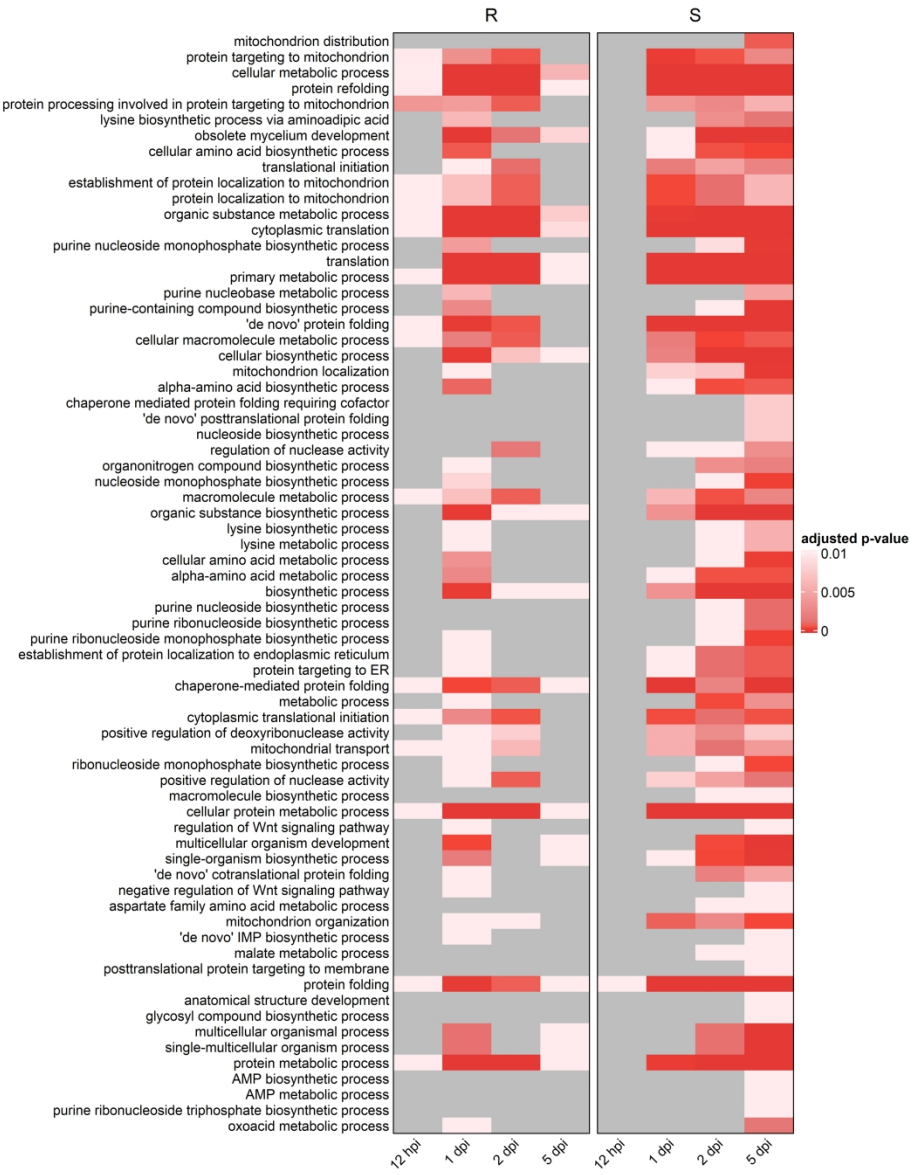

Fig. 2. Over-represented gene ontologies (GO) in the biological processes (BP) category of total expressed Austropuccinia psidii genes in both the R- and S-interaction over the time series, where the colour scale represents the false discovery rate (FDR) adjusted p-value and grey represents absence of the term. GO analysis identified 188 over-represented BP terms, the heatmap represents the top 70 terms in relation to the lowest FDR value. R = resistant interaction; S = susceptible interaction; hpi = hours post inoculation; dpi = days post inoculation.

879x1128mm (96 x 96 DPI)

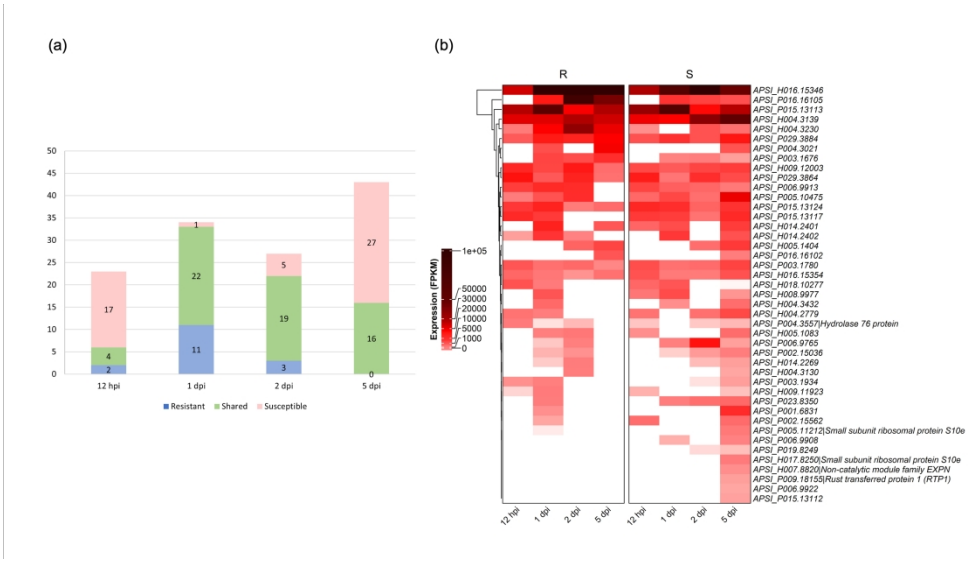

Fig. 3. The expression of Austropuccinia psidii effector genes. (A) The number of expressed Austropuccinia psidii candidate effectors. Blue represents the genes expressed in the R-interaction, green represents expressed genes between the R- and S-interaction, and pink represents effector genes expressed in the S-interaction. (B) The expression of patterns of Austropuccinia psidii effectors genes in both the resistant and susceptible Eucalyptus grandis interactions over the time series. Genes with known annotations are labelled. The colour gradient represents the expression values of a measure of FPKM ranging from the minimum to maximum expression values, where white represents genes that are not expressed. FPKM = fragments per transcript million; hpi = hours post inoculation; dpi = days post inoculation; R = resistant interaction; S = susceptible interaction.

316x175mm (300 x 300 DPI)

Supplementary Material

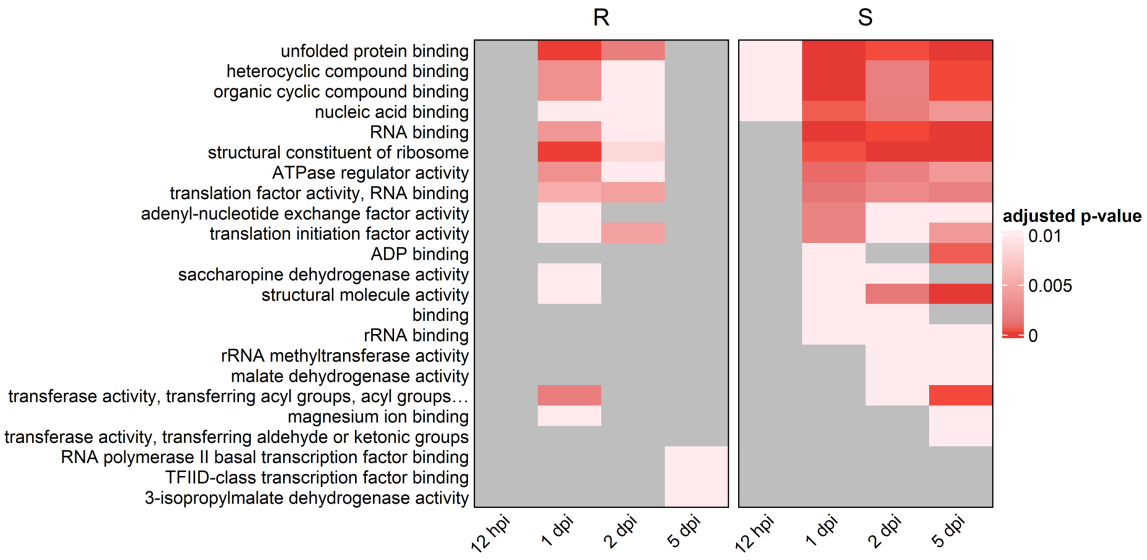

Fig. S1. Over-represented gene ontologies (GO) in the molecular function (MF) category. The heatmap shows enriched terms of the total expressed Austropuccinia psidii genes in both the R- and S-interaction over the time series, where the colour scale represents the false discovery rate (FDR) adjusted p-value and grey represents the absence of the term. GO analysis identified 23 over-represented MF terms. R = resistant interaction; S = susceptible interaction; hpi = hours post inoculation; dpi = days post inoculation.

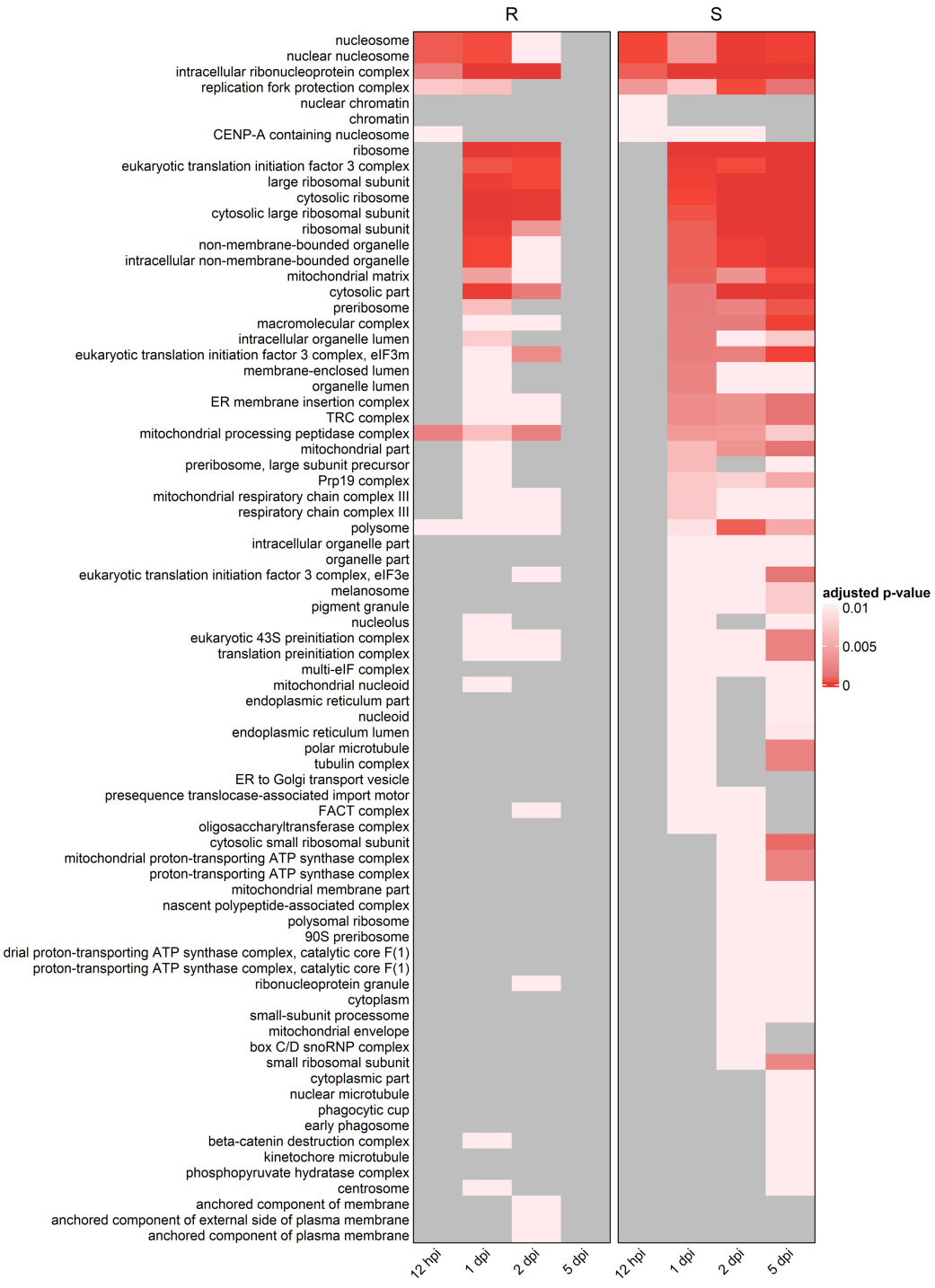

Fig. S2. Over-represented gene ontologies (GO) in the cellular component (CC) category. The heatmap shows enriched terms of the total expressed Austropuccinia psidii genes in both the R- and S-interaction over the time series, where the colour scale represents the false discovery rate (FDR) adjusted p-value and grey represents the absence of the term. GO analysis

identified 77 over-represented CC terms. R = resistant interaction; S = susceptible interaction; hpi = hours post inoculation; dpi = days post inoculation.